# Investigation of Primary Reactions and Secondary Effects from the Pyrolysis of Different Celluloses

Jing Zhang,[†] Michael W. Nolte,[†] and Brent H. Shanks*[,†,‡]

[†]Department of Chemical and Biological Engineering, Iowa State University, 2114 Sweeney Hall, Ames, Iowa 50011, United States
[‡]Center for Biorenewable Chemicals (CBiRC), Iowa State University, 1140 BRL, Ames, Iowa 50011, United States

S *Supporting Information*

ABSTRACT: The primary reactions and secondary effects resulting from cellulose fast pyrolysis were investigated using a micropyrolyzer system by changing sample weight and length scale. To exclude the catalytic effects from metal ions, all cellulose samples were demineralized prior to pyrolysis. Heat transfer calculations estimated the characteristic time scale for heat transfer to be 1 order of magnitude smaller than the pyrolysis reaction time when the sample weight was less than 800 μg. It was found that mass transfer limitations existed when the sample weight of the powder cellulose was larger than 800 μg or when the cellulose particles were pyrolyzed at a larger characteristic length scale. The mass transfer limited system led to secondary reactions including secondary char and gas formation from volatile products and decomposition/dehydration of levoglucosan into low molecular weight products, furans, and dehydrated pyranose. The secondary reactions were found to be catalyzed by the char from cellulose pyrolysis. The pyrolysis of powder celluloses of differing crystallinity, degree of polymerization, and feedstock type were studied. Over 87 wt % mass balance closure was achieved for each type of cellulose. Similar product distributions were obtained for all of the different celluloses, implying that the primary products from cellulose were not influenced by these factors.

KEYWORDS: Cellulose pyrolysis, Crystallinity, Heat/mass transfer, Primary reactions, Secondary effects
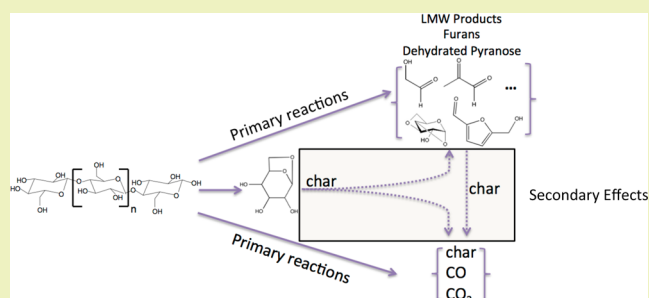
INTRODUCTION

As a route for converting biomass into fuels, fast pyrolysis has unique advantages with one being that it can produce a liquid product, bio-oil, from solid biomass. The process is potentially efficient and environmental friendly due to its short reaction time and low or even neutral emission of greenhouse gases.[1] However, bio-oil has some undesirable characteristics, such as low pH value, low heating value, and relative instability that leads to an inability to directly replace crude oil. The undesired features come from the intrinsically complex chemical composition of bio-oil, which includes a high oxygen content and a multitude of chemical functionality.[1] As such, unraveling the convoluted mechanisms of fast pyrolysis requires detailed chemical speciation of the bio-oil products. Insights into the chemistry involved in fast pyrolysis could help to optimize the fast pyrolysis process, thereby tuning the final product distribution and providing the basis for determining promising downstream upgrading strategies.

Cellulose is a polysaccharide made of D-glucose units connected via β-1−4 glycosidic bonds. It generally makes up to 22−50% by dry mass of a plant, with the value varying for different types of biomass.[1,2] Previous studies have reported the cellulose pyrolysis product distribution with high mass balance closure by using an online micropyrolyzer gas chromatograph (GC)-mass spectrometer (MS)/flame ionized detector (FID) system and infrared (IR) gas analyzer.[3,4] Under fast pyrolysis

conditions, the competitive reaction pathways involved in the primary thermal deconstruction have been proposed, which broadly consist of either the release of levoglucosan or the generation of furans and low molecular weight (LMW) species.[4,5] Recently, Broadbelt et al. have proposed that the primary thermal deconstruction of cellulose to levoglucosan occurred predominantly via a concerted mechanism.[6,7] The computational study suggested that this concerted mechanism was favored kinetically. Previous studies also showed that alkali and alkaline earth metal ions naturally present in biomass altered the cellulose pyrolysis product distribution possibly by changing the activation energy of competing reactions that led to enhancement in the formation of furans and LMW compounds at the expense of levoglucosan yield, even when these metal ions were present at a low level.[5]

Fast pyrolysis is characterized as occurring at a moderate temperature (400−600 °C) with a high heating rate (>500 °C/s). However, there is significant debate on whether specific fast pyrolysis systems are free of heat/mass transfer limitations and what secondary reactions will derive from the transport limitations. Under fast pyrolysis conditions, there will be the existence of different physical processes that each require

consideration, including chemical reactions (kinetics), volatilization and partial pressures of products (mass transfer and thermodynamics), and heating rates and temperatures (heat transfer). For example, it has been commonly known that a thermogravimetric analyzer (TGA) is limited in the heating rates that can be applied. As such, TGA cellulose will begin breaking down at 300–350 °C, thereby producing significant amounts of levoglucosan.[4,8] However, at these lower temperatures, the volatility of levoglucosan will be lower, and as a result, not all of the levoglucosan will escape the heated reaction zone before it further reacts to form oligomers or breaks down to lower molecular weight products and gases unless a sufficiently small sample size and high gas flow rate is applied.[9–11] Therefore, kinetic models based on TGA experiments tend to include reaction rate constants that contain a convolution of the kinetics with the mass and heat transfer effects if the experimental conditions are not carefully controlled. Micropyrolyzers, such as provided by Frontier Laboratories (Japan) or CDS Analytical pyroprobes (U.S.A.), are widely used for fast pyrolysis studies because of the high heating rates, and by extension high reaction and volatilization rates, which can be achieved. Heat and mass transfer depend on various factors in a pyrolysis system, including sample weight, size, physical properties, reactor configuration, type and flow rate of the carrier gas, etc. Therefore, in situ heat and mass transfer situations should be determined at the relevant experimental conditions.

Lin et al. proposed a kinetic model for cellulose pyrolysis in a Pyroprobe, consisting of the formation of levoglucosan, isomerization/dehydration of levoglucosan into anhydrosugars, and oligomerization/decomposition of the anhydrosugars to oligomers/LMW.[12] However, it is likely that this mechanism includes both primary and secondary reactions because the residence time of vapor products could be several seconds or even longer in such a system. Patwardhan et al. studied primary and secondary reactions for cellulose fast pyrolysis by comparing product distributions from a micropyrolyzer and a fluidized bed reactor, the latter of which has a much longer residence time.[13] Oligomerization of levoglucosan upon condensation and decomposition of dehydrated pyranoses and furans into LMW and gases were proposed to be secondary reactions.[13] However, individual experiments using model compounds under comparable reaction conditions have not been performed to further validate the claim. Mettler et al. proposed a pyrolysis model of thin film cellulose made from powdered cellulose with a characteristic length scale claimed to be 3 μm. The calculated heating rate for the thin film was greater than 1,000,000 °C/min under typical pyrolysis temperatures in the micropyrolyzer system. Unlike the pyrolysis of powder cellulose, the thin film model was claimed to be free of heat and mass transfer limitation, but it gave a lower yield of levoglucosan and a higher yield of LMW and char.[3,14] Interestingly, Mettler et al. also proposed dehydration/decomposition of levoglucosan into anhydrosugars and LMW as secondary reactions, which seems to contradict the lower levoglucosan yield and higher LMW yield from the thin film cellulose than powder cellulose.[15] Patwardhan et al. tested cellulose with particle sizes of 20 and 50 μm and sample weights ranging from 200 to 800 μg in a Frontier Lab micropyrolyzer and found no significant difference in product distribution, thereby concluding that heat and mass transfer effects did not change within the tested range.[4] However, a systematic evaluation of heat and mass transfer limitations with

a broader range of sample weight and cellulose morphology would be useful.

Two other important properties that may be considered are the crystallinity and degree of polymerization (DP). The crystallinity is important because it reveals the degree to which the polysaccharide strands are packed relative to each other and the amount of hydrogen-bonding between separate strands.[16] The DP will depend not only on the type of biomass from which the cellulose is isolated but also on the isolation and pretreatment method.[17]

The influence of crystallinity and DP on cellulose pyrolysis has been studied with the primary focus on constructing kinetic models for different celluloses and then comparing parameter differences between the experimental results and proposed models.[8,18–21] Schultz et al. postulated that the crystallinity affected the enthalpy and entropy changes in different celluloses and, in turn, affected the rate constants and activation energy within their pyrolysis kinetic model.[20] Poletto et al. reported that the cellulose crystallite size influenced both the activation energy and thermal stability during the cellulose thermal decomposition.[19] In contrast, Kim et al. suggested that neither crystallite size nor crystallinity affected the activation energy during the thermal decomposition of cellulose.[21]

The initial thermal degradation temperature (T_i) has also been proposed as being a characteristic determined by the crystallinity and DP of cellulose. Several groups have suggested that cellulose with a lower crystallinity and shorter polymeric chain length would have lower T_i values.[8,18,20] Also, thermal glycosidic bond cleavage has been proposed to preferentially occur in the amorphous regions of cellulose due to fewer hydrogen bonds and diminished van der Waals forces.[22]

It is important to note, however, that most of these studies were performed in a TGA, which cannot create the high heating rates necessary for high reaction and product volatilization rates in fast pyrolysis. Additionally, the analysis methodology used was primarily based on sample weight loss leading to an inability to comprehensively compare product distributions. Recently, Wang et al. studied the influence of crystallinity on cellulose pyrolysis by using a Pyroprobe with online GC-MS analysis and reported that cellulose with lower crystallinity tended to form less levoglucosan and more furans.[23] However, as was the case with a number of the above-mentioned articles, sample purity data with respect to mineral content was not shown, which has been shown to be crucial in cellulose thermal decomposition. Moreover, heat and mass transfer limitations could be convoluted with crystallinity effects because their ball-milled lower crystallinity cellulose would have a smaller particle size. Cellulose samples with different particle sizes could have different heat and mass transfer behavior particularly under the relatively low heating rate of 100 °C/s applied in the Wang et al. work.

In the current work, all cellulose samples were pyrolyzed with an online micropyrolyzer GC-MS/FID system. Theoretical calculations for the heating rates within the micropyrolyzer were performed under the specific experimental conditions to determine if the micropyrolyzer is capable of providing fast pyrolysis reaction conditions. Prior to pyrolysis, all samples were validated to have low mineral concentrations so as to exclude the confounding catalytic effects from metal ions. The primary and secondary reactions during cellulose fast pyrolysis were systematically evaluated by changing sample weight, particle size, and morphology of cellulose samples. Pyrolysis of model compounds under suspected secondary reaction

conditions was performed to validate secondary reactions. The goal of the current work was to reconcile the apparent inconsistencies reported in the literature for cellulose pyrolysis by investigating various cellulose properties to find the effect on pyrolysis product distribution. Namely, celluloses with different particle sizes, crystallinities, and degrees of polymerization, as well as from different feedstocks were analyzed. Additionally, the effect of sample mass and pyrolysis temperature were investigated.

■ EXPERIMENTAL METHOD

Materials. Sigmacell 20, Sigmacell 50, Avicel PH-101, and Whatman 542 filter paper celluloses were purchased from Sigma-Aldrich. The Whatman 542 filter paper was ball milled into a powder form prior to pyrolysis. Phosphoric acid swollen cellulose (PASC) was provided by the National Renewable Energy Laboratory (NREL), which was produced from Sigmacell 50 cellulose using the method of Zhang et al.[24] Nanocellulose, as a 2% solution of cellulose microfibrils (1−2 μm long and 5−20 nm in diameter) in water, was kindly provided by Innventia (Stockholm, Sweden). Alpha-Cel BH100, Alpha-Cel BH200, JustFiber BF200, and JustFiber WWF200 were received from the International Fiber Corporation.

Sample Preparation and Characterization. The mineral content of the cellulose samples was analyzed by inductively coupled plasma mass spectrometry (ICP-MS). For the cellulose samples whose mineral content was excessive, acid washing or water washing was performed until a sufficiently low mineral level was achieved. Scanning electron micrographs (SEM) were obtained using a FEI Quanta FE-SEM. The DP and crystallinity index for the cellulose samples were determined by gel filtration chromatograph (GFC) and X-ray diffraction (XRD), respectively. Experimental details are given in the Supporting Information.

Pyrolyzer GC-MS/FID. Fast pyrolysis was performed on a single-shot micropyrolyzer (model 2020iS, Frontier Laboratories, Japan). A total of 200−500 μg of sample (unless otherwise noted) was loaded into a deactivated stainless steel cup. For analysis, the sample-containing cups were dropped into the preheated reaction zone. For a standard experiment, a 500 °C pyrolysis temperature was used with 100 mL/min of helium flow as a sweep gas (100:1 split ratio). Volatilized products were swept through the reaction zone into the pyrolyzer injection needle (at 320 °C), the gas chromatograph (GC) injection port (300 °C), and finally into the GC column. The GC separation was performed using a medium polarity ZB-1701 column (Phenomenex, 86% dimethylpolysiloxane, 14% cyanopropylphenyl), and a temperature program that started at 50 °C, heated at 5 °C/min to 300 °C, and held at 300 °C for 5 min. Pyrolysis products were identified using a mass spectrometer (MS, Varian Saturn 2000) and quantified with a flame ionization detector (FID, Bruker 430-GC) after confirmation and calibration with pure standards, the details of which can be found in the Supporting Information. A near-infrared gas analyzer (DeJaye, Des Moines, U.S.A.) was used to quantify CO and CO_2 yields, while char yields were quantified by taking the difference in weight of the sample cup before and after pyrolysis. Each experiment with error bars was run in triplicate with the error bars indicating one standard deviation.

■ RESULTS AND DISCUSSION

Estimating Micropyrolyzer Heating Rate. Sample heating rates are crucial parameters to evaluate heat transfer limitations inside of the pyrolysis reaction system. The rates are controlled by various factors, such as sample weight, sweep gas flow rate, pyrolysis temperature, configuration of pyrolyzer, etc. Because heating rates are determined by specific experimental conditions, the heating rate calculations must be performed for those precise conditions. Several articles calculated the heating rates for biomass fast pyrolysis, but failed to consider certain details,[3,14] such as whether the inert gas has been heated up to

reaction temperature before contacting the biomass or if the heating rate of biomass is higher than the pyrolysis cup. Additionally, the convective heat transfer coefficient needed to be determined under experimental conditions. To address these issues, a systematic calculation was performed in the current study with a reaction temperature of 500 °C and a helium flow rate of 103 mL/min.

Figure 1 shows the configuration of the micropyrolyzer used in the current study. Full data for the length scale of the
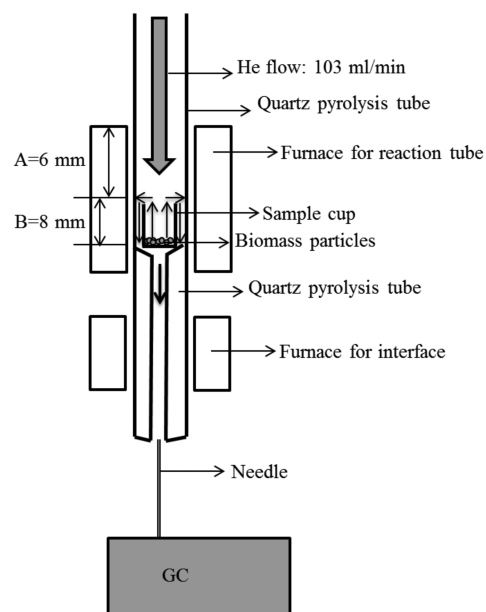

Figure 1. Configuration of the micropyrolyzer.

micropyrolyzer and physical properties are given in the Supporting Information. The convective and radiative heat transfer from the quartz tube to the helium were used to calculate the heating rate of the helium. The Nusselt number was calculated using the empirical formula for forced convection in laminar pipe flow[25] and was subsequently used to calculate the convective heat transfer coefficient. It was found that under the experimental conditions, the helium only needed 1.2 mm to be heated to reaction temperature after entering the furnace zone, which was a much shorter distance than the depth of the cup (length A, Figure 1). Therefore, the helium reaching the cup and sample was at 500 °C. Detailed calculations for heating rates, Biot number, and the assumptions made during the calculation are shown in the Supporting Information.

The modes of heat transfer to the cup include both convective heating from the helium and radiative heating from the quartz tube. The same empirical formula was applied to calculate the Nusselt number considering both the inside and outside of the cup. The initial temperature of the cup was taken as 25 °C. The temperature versus time plot for the cup resulted from a numerical solution of the heat transfer differential equation (Figure 2A). The heating rate for the cellulose sample was calculated by assuming the heat transfer was primarily due to convective heating from the helium instead of conductive heating from the cup. For powder cellulose, the average Nusselt number was calculated using the empirical formula for a flat plate in laminar flow because the powder cellulose was located on the bottom of the cup.[26] The same empirical formula was
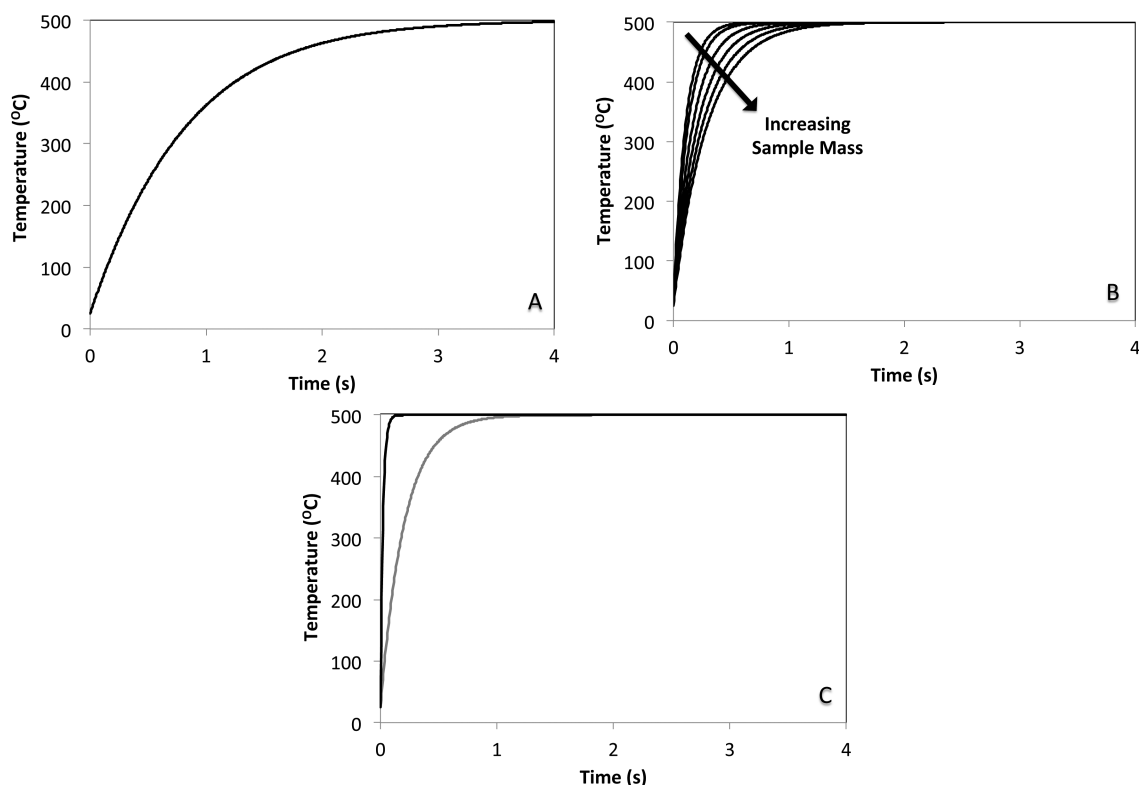
Figure 2. Estimated heating rates in the micropyrolyzer to 500 °C. (A) Heating rate of an empty pyrolysis cup. (B) Heating rate of powder cellulose at masses of 250, 300, 400, 500, 600, and 700 μg. (C) Heating rate of 250 μg of thin film cellulose of either 2 μm thickness (nanocellulose slurry, black) or 100 μm thickness (powder cellulose, gray).

used for the thin film from powder cellulose because the majority of cellulose was located on the bottom of the cup with a thickness around 100 μm. For the thin film from nanocellulose, a thickness of 2 μm was chosen to represent the average length.

Figure 2 shows the temperature vs time for the cup, powdered cellulose, and thin film cellulose, which found that the heating rate of the cellulose was higher than the cup. Figure 2B and C show cellulose samples approached the reaction temperature within 1 s, which is less than characteristic reaction time scale from 2.5 to 3 s as predicted by a microkinetic model from Vinu and Broadbelt.[6] Therefore, the calculations supported the conclusion that both thin film cellulose and powder cellulose were heated to reaction temperature before the pyrolysis reactions were completed.

Effect of Particle Size and Sample Mass. Cellulose was pelletized using a Carver, Inc. pellet press (40,000 lb$_f$ for 3 min). The large cellulose pellet was broken apart and sieved to specified sizes (Figure 3). The levoglucosan yield for the commercially available celluloses (20 and 50 μm size particle) was similar, 58.4 and 55.5 wt %, respectively, and comparable with a previous study.[4] On the basis of the Tukey honest significant difference test (HSD), as the particle size was increased and sample mass was held below 800 μg, there were no significant deviations in levoglucosan yield. Even at the largest tested particle size, at over an order of magnitude larger (850−1000 μm), there was no significant change in levoglucosan yield.

If significant heat transfer limitations existed, the particle interior would be at a lower temperature than the exterior. When pyrolyzing cellulose at different temperatures, a higher levoglucosan yield was found at a relatively lower temperature
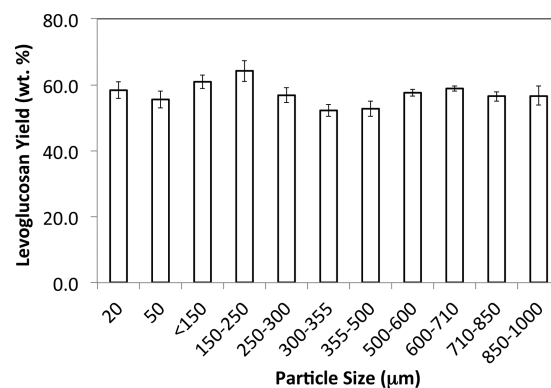

Figure 3. Levoglucosan yield (wt %) from different particle sizes of cellulose. The 20 and 50 μm samples are Sigmacell 20 and Sigmacell 50, respectively. The remaining particle sizes are from pelletized Sigmacell 50.

(Figure 4). As such, a higher levoglucosan yield may be anticipated in particles with temperature gradients present. For example, if a larger particle underwent pyrolysis while having an exterior temperature close to 500 °C while the interior temperature was lower, the overall levoglucosan yield should have increased. However, as demonstrated in Figure 3, a correlation of particle size within the range tested with the levoglucosan yield was not observed

Heat transfer limitations could also arise if the cellulose sample mass becomes too large as a larger sample mass would require a longer heating time to reach pyrolysis temperature under heat transfer limitation. This would lead to a portion of the cellulose undergoing pyrolysis at lower temperatures. To test for the sample size effect, the cellulose sample mass was
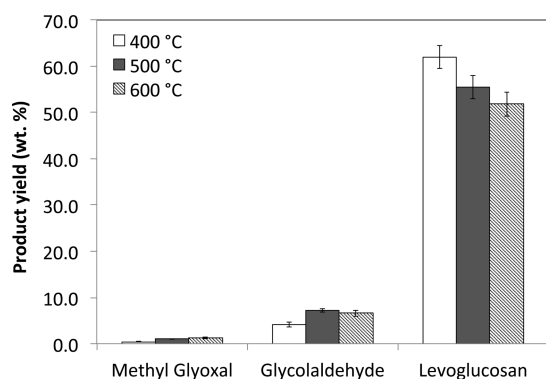
Figure 4. Comparison of methyl glyoxal, glycolaldehyde, and levoglucosan yields (wt %) at different cellulose pyrolysis temperatures.

increased from the conventional range of 200−500 μg up to 2000 μg (Figure 5). From comparing the yield of levoglucosan and total GC detectables, it is shown that the yields gradually decreased when the sample mass was increased above 800 μg. Therefore, the larger samples seemed to be limited by mass transfer rather than heat transfer because the yield of levoglucosan went down instead of up, possibly due to the fact that levoglucosan could not escape rapidly enough from the reaction zone. The same trend was observed for the major LMW products, i.e., methyl glyoxal, glycolaldehyde, or 5-hydromethylfurfural (5-HMF), among others. In contrast, the yield of gases, CO and CO_2, and char increased when a large sample weight (>1000 μg) was used.

Thin Film Cellulose Pyrolysis. The length scale and compositional identification of thin films made from nanocellulose and Sigmacell 50 were measured using SEM (Figure 6). Four compositional regimes were identified by EDS: cellulose, epoxy-iodoform, Si−O, and the steel cup (Figure 6A and D). The full details on the EDS result for the phase identification is given in the Supporting Information. The distribution and morphology of the cellulose within the pyrolysis cup was different between Sigmacell 50 and nanocellulose. For the thin film prepared from the nanocellulose slurry, a continuous film was observed on the wall of the pyrolysis cup with a thickness of several microns (Figure 6D and E). A negligible amount of cellulose was found at the bottom of the cup (Figure 6F). In contrast, the synthesis procedure with the Sigmacell 50 resulted in a thin film with a discontinuous distribution of particles or clumps on the wall instead of a thin film. The thickness of these clumps is also several microns (Figure 6A and B). Unlike the thin film prepared from the nanocellulose slurry, most of the Sigmacell

50 was deposited as a layer at the bottom of the cup with a thickness around 100 μm (Figure 6C). The suspended Sigmacell 50 primarily fell out of solution and deposited on the bottom of the cup during drying, while the nanocellulose slurry had a high enough yield stress to remain on the wall. Therefore, a continuous thin film of several microns was only formed using the nanocellulose slurry, while the powdered cellulose formed one or several large cellulose agglomerations on the bottom of the cup measuring about 4 mm in diameter and 100 μm in thickness. To be consistent, the "thin film" from the Sigmacell 50 powder cellulose will be hereinafter referred to as a thin film.

Pyrolysis of the nanocellulose-generated thin film had a similar product distribution to Sigmacell 50, the standard powdered cellulose (Figure 7 and Table S6, Supporting Information). However, a difference was observed when a thin film of Sigmacell 50 (thin film, made from powder cellulose, Figure 7) was pyrolyzed. For this sample, a higher yield for LMW, furans, gas, and char, and a lower yield for levoglucosan was observed. Because all cellulose samples were demonstrated to have a negligible amount of metal ions, the difference in product distribution should be attributable to transport limitations. The thin film from the nanocellulose slurry was the most likely to be free of mass and heat transfer limitations due to it having the smallest length scale with regard to mass transfer and the largest surface area for convective heat convection.

According to the heat transfer calculations, 0.3 s would be needed to heat 250 μg of powder cellulose to 500 °C (Figure 2B). The results for the nanocellulose and powder cellulose thin films would be 0.1 and 0.6 s, respectively, to attain 500 °C (Figure 2C). Importantly, the heating time estimations were less than the characteristic reaction time scale from 2.5 to 3 s for cellulose fast pyrolysis.[6] Moreover, if heat transfer limitations were present, part of the cellulose would actually be pyrolyzed at a lower temperature than 500 °C, which contrary to the actual results would lead to a higher yield for levoglucosan and a lower yield for LMW as discussed in the previous section. Therefore, it did not appear that heat transfer effects were responsible for the change in the product distribution that was observed.

Considering the different length scales for these three cellulose samples, mass transfer effects could be a cause of the product distribution differences. The thickness of the thin film formed from the nanocellulose slurry was shown to be around 2 to 4 μm (Figure 6E). On the other hand, the thin film from the powder cellulose formed a large mass covering the bottom of the cup with a thickness around 100 μm. The dimension of the powder cellulose was approximately 50 μm × 10 μm × 10 μm.
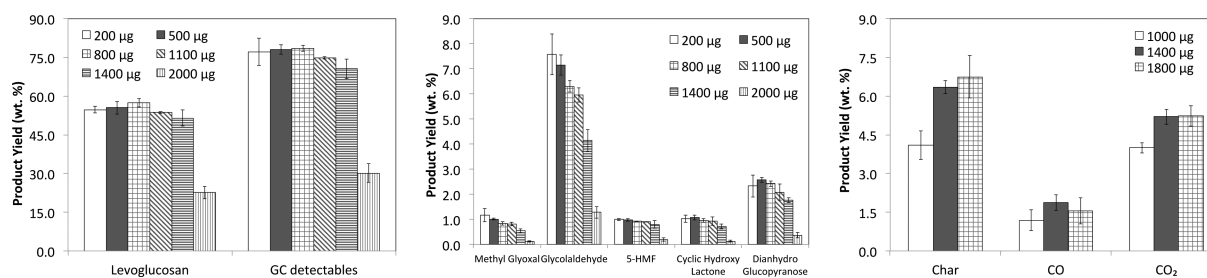

Figure 5. Yields (wt %) of levoglucosan and the total GC detectables (left figure), and methyl glyoxal, glycolaldehyde, 5-HMF, cyclic hydroxy lactone, and dianhydro glucopyranose (center figure), and char, CO, and CO_2 (right figure) from the pyrolysis of different masses of cellulose.
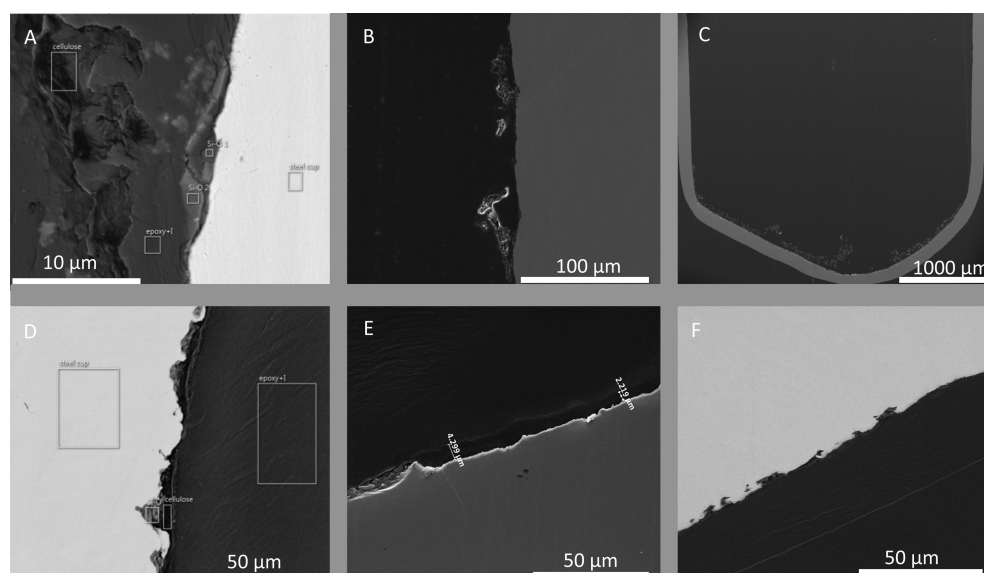
Figure 6. SEM-EDS cross sectional images of the pyrolysis cup coated with thin film cellulose: (A) phase identification of thin film from Sigmacell 50 on the wall, (B) thin film from Sigmacell 50 on the wall, (C) thin film from Sigmacell 50 on the bottom, (D) phase identification of thin film from nanocellulose on the wall, (E) thin film from nanocellulose on the wall, and (F) thin film from nanocellulose on the bottom.
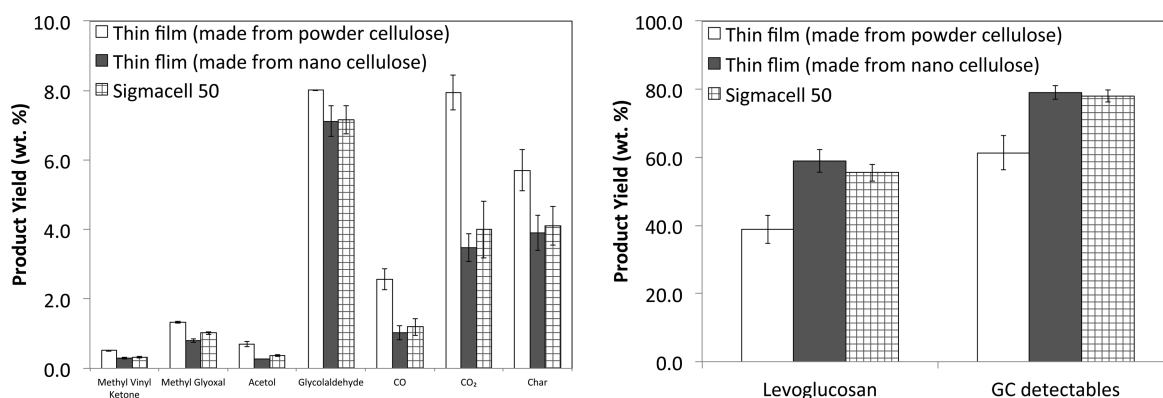

Figure 7. Comparison of major products yields from two different thin film celluloses and powder cellulose (Sigmacell 50) (full product distribution is available in the Supporting Information).

The similarity in product distributions between the powder cellulose and the nanocellulose thin film suggested that the powder cellulose had negligible mass transfer limitations if the proper sample weight was used. For the powder cellulose thin film, the sedimentation of the powder and elimination of the void space among the cellulose particles during drying led to the formation of a large cellulose clump at the sample cup bottom that could have increased mass transfer resistance. However, it should be noticed that the change in product distribution for the powder cellulose thin film was not consistent with the one observed by excessive sample weight, which led to lower yields for both levoglucosan and LMWs/furans.

Pathways for Levoglucosan Formation. During cellulose pyrolysis, once levoglucosan has been formed, it may either volatilize and escape the high-temperature reaction zone or it may further react to form char or LMW products. It was shown previously that a thin film of cellulose will produce less levoglucosan than powdered cellulose.[3] The lower levoglucosan yield from thin film pyrolysis may be related to its low volatility. The vapor pressure of levoglucosan at room temperature (25 °C) was estimated to be 9×10^{-5} Pa by extrapolating from the

experimental values of Oja and Suuberg.[27] This vapor pressure is significantly lower than another high boiling pyrolysis product, 5-HMF (0.08 Pa),[28] and it is much lower than the vapor pressures for key LMW products, namely, acetol (500 Pa),[29] acetone (30,000 Pa),[30] or glycolaldehyde (5 Pa).[29] In addition, Bai et al. tested levoglucosan volatility by pyrolyzing cellulose in covered TGA cups, and it was found that as the pressure inside the cup was increased (by using fewer holes in the cup cover) and levoglucosan yield was decreased, while oligomer (char) yields increased.[9] Therefore, reduced opportunity for the levoglucosan to volatilize will hinder its ability to escape from the reaction zone, and in turn, it will increasingly form char or breakdown to LMW products.

To examine the extent to which levoglucosan volatility affects its pyrolysis yield in the current experimental apparatus, two different experiments were performed. The first experiment was similar to that reported in Figure 5 with an increasing mass of powdered levoglucosan from 200 μg up to 2000 μg being pyrolyzed. By increasing the sample mass, the partial pressure of levoglucosan within the reaction zone was increased. The second experiment involved creating a thin film of levoglucosan (200 μg) on the bottom of the pyrolysis cup, thereby creating a

high localized partial pressure. In both experiments, ~100% of levoglucosan was recovered with negligible degradation to char or LMW products. Therefore, these two experiments did not create sufficiently high levoglucosan partial pressure to impact its recovery.

To examine whether a higher levoglucosan partial pressure in the presence of other pyrolysis products could lead to degradation, cellulose and levoglucosan were copyrolyzed. In this experiment, about equal masses of cellulose and levoglucosan (with a total mass <800 μg) were mixed together and subsequently pyrolyzed. A levoglucosan yield of ~76 wt % was obtained, equal to ~100 wt % yield from the pure levoglucosan and ~55 wt % yield from cellulose, indicating there was no interaction effects.

A second set of experiments were performed in which levoglucosan and cellulose char were copyrolyzed at a ratio of 10:1 LG:char by mass using different sample weights (Figure 8). When 600 μg of LG was pyrolyzed with ~60 μg of char,
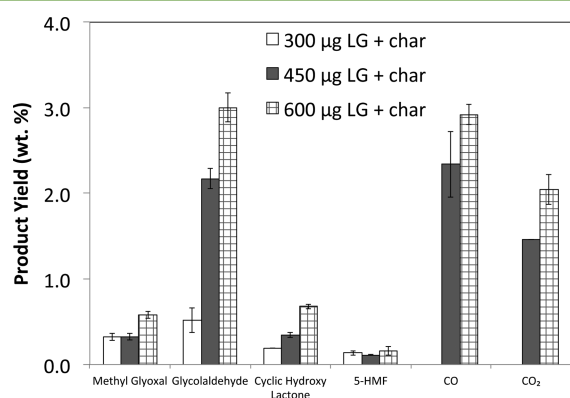

Figure 8. Yields (wt %) of major low molecular weight products, gases, and solids from the copyrolysis of levoglucosan and char at a 10:1 mass ratio.

only about 50 wt % of the levoglucosan was recovered. A considerable amount of gases, LMW, furans, dehydrated pyranose, and char were generated at the expense of levoglucosan yield when a large sample weight was used. Few secondary products were produced from the copyrolysis when the levoglucosan weight was less than 300 μg. A negligible amount of secondary products were generated when pyrolyzing levoglucosan alone with sample weights ranging from 200 to 800 μg. Therefore, the char appeared to catalyze the decomposition and dehydration of levoglucosan into gases, LMW, furans, dehydrated pyranose, and additional char if the sample weight of levoglucosan and char was sufficiently large. The catalytic effect of the char was also investigated with cellulose. At a mass ratio of 5:1 cellulose:char (500 μg cellulose and 100 μg char), the levoglucosan yield decreased to ~47 wt % from 55 wt % for the pure case.

To evaluate secondary reactions from the LMWs and furans, the copyrolysis of the glycolaldehyde dimer and 5-HMF with char was performed using a ratio of 1:1. The glycolaldehyde dimer was used due to the lack of commercially available pure glycolaldehyde. Previous work showed that glycolaldehyde dimer pyrolysis at 500 °C generates a single major peak representing glycolaldehyde in the pyrolyzer GC-MS system.[4] For sample weights less than or equal to 50 μg, almost all of the glycolaldehyde dimer was converted into glycolaldehyde. With an increasing sample weight, the yield of glycolaldehyde

decreased, which was accompanied by the formation of CO and CO_2. It was not possible to quantify the gas yield when the sample weight is less than 500 μg due to the sensitivity of the IR detector. Therefore, the gas yield is only shown for sample weights larger than 500 μg. A poor mass balance was obtained for the higher sample weights, possibly due to species condensing in the transfer line to the GC column and/or the formation of undetectable gases. Similarly, the formation of CO and CO_2 was observed from the copyrolysis of 5-HMF with char for sample weights larger than 500 μg. Additionally, secondary char formation was detected, the yield of which increases with increasing sample weight. Similar to glycolaldehyde, the yield of 5-HMF decreases with increasing sample weight. Therefore, it appeared secondary reactions from LMWs and furans to form CO, CO_2, and secondary char occurred for higher sample weights in the presence of char.

As lower yields of levoglucosan, furans, and LMWs and a higher yield of char and gases were observed during the pyrolysis of powder cellulose at higher sample weights, the change in yields may be caused by the interaction of levoglucosan, furans, and LMWs with the primary char, leading to the formation of secondary gases, char, or LMW products (Figure 9). The powder cellulose thin film generated a lower
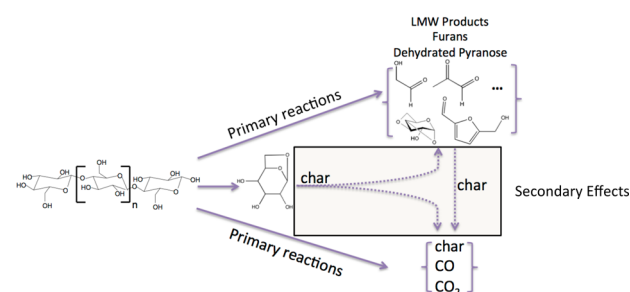

Figure 9. Primary and secondary reactions during cellulose fast pyrolysis.

yield of levoglucosan and a higher yield of gases, LMW, furans, and char, even when relatively low cellulose sample weights were used. This result was directionally similar to the impact of char on the pyrolysis. For the powder cellulose thin film system, the larger clumps were coupled with less void spacing and more intimate contact between the cellulose particles. Therefore, as char was formed during pyrolysis, there may be an increased amount of contact and interaction between the pyrolysis vapors, unreacted cellulose, and char within the more closely packed system. The increased contact might have enhanced the char-forming reactions or other degradation reactions. This increased char, gas, and LMW formation would come at the expense of levoglucosan and other low volatility products. As a result, GC detectable yields would be lower and char yield would be increased, as shown from the experimental data.

Effect of Crystallinity, Chain Length, and Feedstock. Shown in Figure 10 are XRD patterns for a number of cellulose samples. The PASC and ball-milled Whatman 542 are clearly amorphous, as demonstrated by the broad peaks ranging from 9 to 30 2θ and the absence of characteristic peaks for crystalline cellulose (Figure 10). The maximum intensity was around 19.45 2θ, which is consistent with the powder diffraction file (PDF) database for amorphous cellulose. The other six cellulose samples gave XRD patterns that were similar to cellulose type I$_\beta$ (Figure 10). Five characteristic peaks or peak
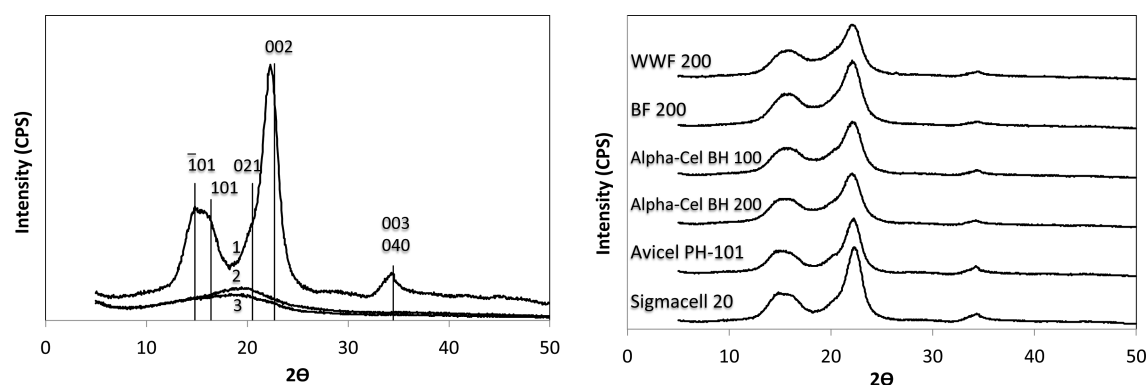
Figure 10. XRD patterns for different celluloses: (a) comparison of Sigmacell 20 (1) with two amorphous celluloses (PASC (2) and ball-milled Whatman 542 (3)) and (b) comparison of the six crystalline celluloses.

shoulders, with crystal lattice assignments of $(\bar{1}01)$, (101), (021), (002), and (003) or (040), were found for all six of these celluloses.

Many studies have used the crystallinity index to quantitatively describe the degree of crystallinity, but some authors have suggested that the crystallinity index for a specific sample could be different if alternative methodologies are used.[31,32] Therefore, consistent methodologies should be applied to compare crystallinity of different celluloses. In the current study, three methods were applied to calculate the crystallinity of each cellulose sample, including the peak height ratio and two different peak area ratios.

The absolute crystallinity values were different for different calculation methods (Table 1) but were consistent when

Table 1. Crystallinity of Cellulose Samples Calculated by Three Different Methods from XRD

sample	crystallinity (peak height)	crystallinity (peak area)[a]	crystallinity (peak area)[b]
Sigmacell 20	80.4	48.1	58.0
Avicel PH-101	78.9	47.3	57.7
Alpha-Cel BH 100	64.7	36.2	47.8
Alpha-Cel BH 200	65.0	37.4	45.8
BF 200	65.1	36.9	45.7
WWF 200	61.5	33.9	42.1
PASC	0	0	0
ball-milled Whatman 542	0	0	0

[a]By removing air-scattering curve. [b]By removing background.

compared within the same method. The DP of different celluloses was measured by GFC unless otherwise mentioned (Table 2). As shown in Tables 1 and 2, the eight cellulose samples covered a wide range of crystallinity and DP, which provides a good basis for evaluating their influence during fast pyrolysis.

The fast pyrolysis of the different powder celluloses was performed at 500 °C and a sample weight of 500 μg to

investigate the primary reactions in fast pyrolysis. The particle size for each cellulose sample was controlled to around 50 μm. Avicel PH 101, BH 100, BH 200, BF 200, and WWF 200 were used as received because the original size is close to 50 μm and the PASC and ball milled Whatman 542 had to be sieved to obtain 50 μm particles. The product gases, char, and 30 two GC-detectable compounds were identified and quantified. Shown in Figure 11 are parity plots comparing the yields of the quantified pyrolysis products for the celluloses referenced to Sigmacell 50.

As shown in Figure 11, the different celluloses had very similar pyrolysis product distributions to that of Sigmacell 50. From these parity plots, it was evident that the pyrolysis product yields from the eight types of cellulose were quite similar, despite the differences in the feedstock source, crystallinity, and DP (Table S9, Supporting Information). The Tukey honest significant difference (HSD) test was also used to determine whether the product yields from different celluloses were significantly different or not. The results (Table S10, Supporting Information) suggested a statistically equivalent yields for nearly all of the pairwise comparisons among different celluloses, which demonstrated the crystallinity index, DP, and feedstock type had a negligible influence on the resulting product distributions. Whether the cellulose sequence was arranged by crystallinity, DP, or feedstock source, no trend could be found in the yields of a single product, further demonstrating that variation in the crystallinity, DP, or feedstock source does not impact the primary reaction chemistry.

The theoretical water yield was calculated using the stoichiometric amount released from the generation of the dehydration products, such as levoglucosan, furfural, dianhydro xylopyranose (DAXP), 5-HMF, dianhydro glucopyranose, char, etc. For this calculation, the char was assumed to be pure carbon because the elemental analysis on cellulose-derived char showed an approximate molecular formula of $CH_{0.22}O_{0.09}$. The unaccounted portion in the mass balance was most likely due to three sources: (1) low yields of unidentified products in the GC chromatograph, (2) condensed species in the transfer line to

Table 2. Degree of Polymerization for Different Types of Cellulose

cellulose type	Sigmalcell 50	Avicel PH-101	BH 100	BH 200	BF 200	WWF 200	PASC	ball-milled Whatman 542
DP[a]	1871[b]	241[c]	1341	1401	858	858	1712	1334

[a]DP as calculated from the weight-average molecular weight. [b]Measured by National Renewable Energy Laboratory (NREL). [c]Courtesy of Sigma-Aldrich.
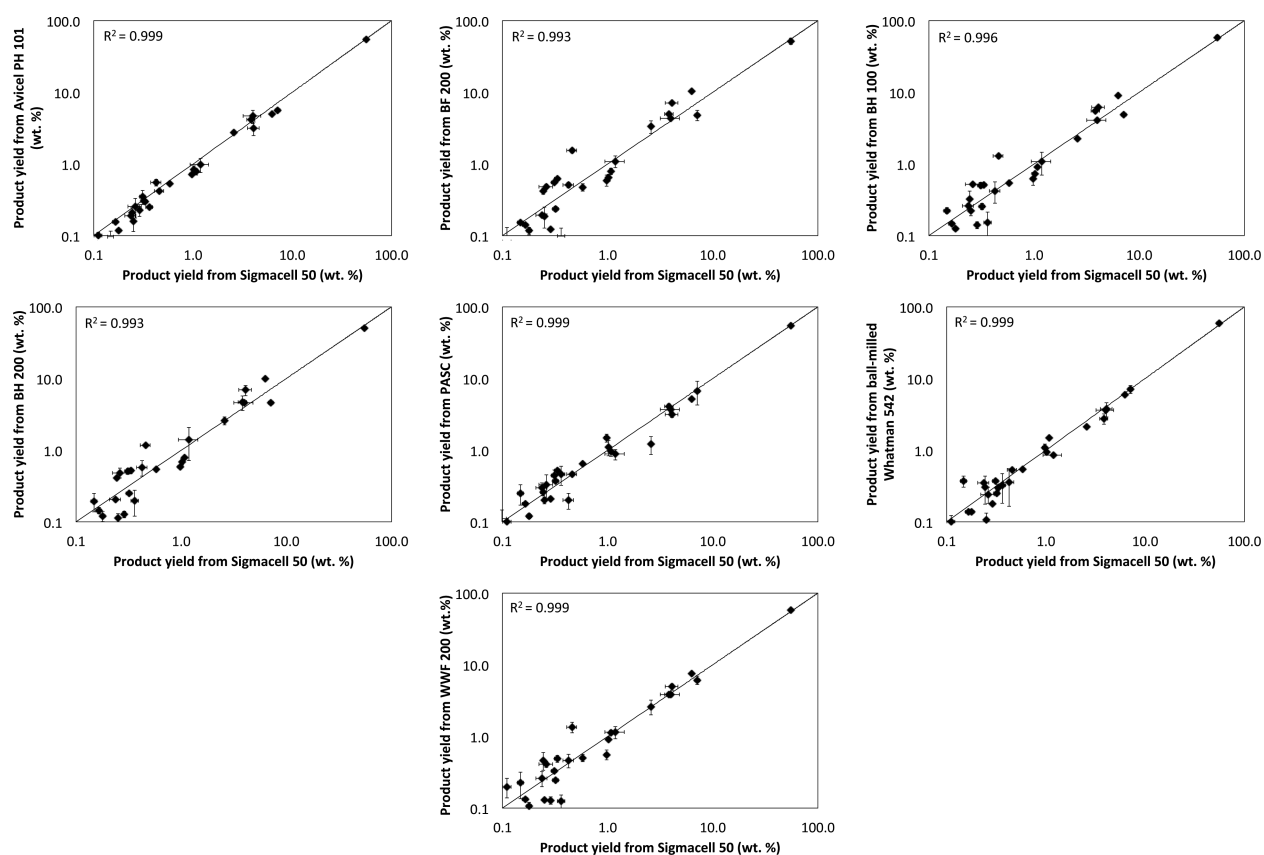
Figure 11. Parity plots comparing the product distributions between Sigmacell 50 and seven other celluloses.
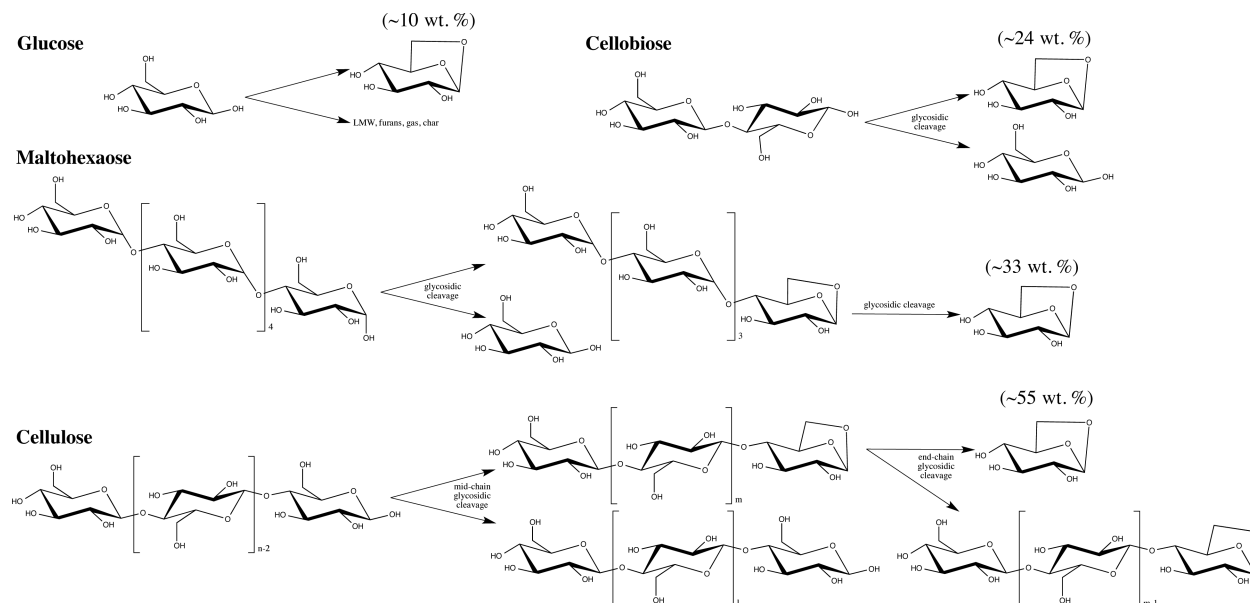

Figure 12. Pyrolytic formation of levoglucosan from glucose-based carbohydrates with different chain lengths.[4,5]

the GC column, and (3) noncondensable gases that could not be detected by the IR-gas analyzer, such as hydrogen and light alkanes.

The glycosidic bonds between glucose units and the hydrogen bonds between hydroxyl groups dictate the degree of crystallization for cellulose.[16] The structure of the crystalline region in cellulose has been proposed to be laterally ordered sheets with a 3-fold anisotropy.[33] van der Waals forces exist perpendicular to these ordered sheets, which further favors the formation of a highly ordered crystalline lattice. In contrast, the extent of hydrogen bonding and van der Waals attraction is significantly less in the amorphous region of cellulose. The carefully controlled hydrolysis used in producing Avicel helps to remove the amorphous portion existing in the starting substrate. While for PASC, the hydrogen bonding network and interlaminar van der Waals forces were disrupted during the

swelling process, leading to a smaller crystalline region and a higher degree of imperfection in the amorphous region. It is well known that the ball milling process can produce amorphous cellulose, which was found from crystallinity measurements on ball-milled Whatman 542.

It has been proposed that the primary reactions in the fast pyrolysis of cellulose consist of competitive pathways.[4,6] In these pathways, glycosidic bond cleavage favors the formation of levoglucosan, while fragmentation of carbon–carbon bonds in the glucosyl ring favor formation of C1 to C3 low molecular weight compounds. The important question explored here was whether the presence of hydrogen bonding and van der Waals forces can perturb this reaction network. It has been speculated by some that the energy required for bond cleavage could be lower for amorphous cellulose than crystalline cellulose. However, it is important to note that the dissociation energy for the glycosidic bond is around 80 kcal/mol, while the energies for hydrogen bonding and the van der Waals force are expected to be about 5 and 2–3 kcal/mol, respectively, making the dissociation energy of H bonds or van der Waals forces smaller by an order of magnitude relative to the glycosidic bonds.[16] As such, the fast pyrolysis conditions of 500 °C with heating rates of about 1000 °C/s appeared to give facile breakage of the hydrogen bonds and van der Waals forces, leading to their presence having at best a weak role in influencing the final product distribution. Kim et al. reported that the degree of crystallinity might be an important factor affecting heat transfer during the thermal decomposition of cellulose because it influenced the initial decomposition temperature.[21] However, heat transfer issues would not be expected to be important in the current study as the reaction system being used was demonstrated to be free of any significant heat transfer or mass transfer effects.[4]

Regarding the DP, previous work had shown that the yield of levoglucosan from fast pyrolysis had the following trend: polysaccharides > oligosaccharides > disaccharides > monosaccharide.[4] This trend was consistent with the proposed thermal deconstruction mechanism in which cleavage of an internal glycosidic bond forms a levoglucosyl end group and a chain with a nonreducing carbohydrate end. In contrast, if the glycosidic bond cleavage occurs at the reducing end group in the polysaccharide chain, a chain is created with a levoglucosyl end group and one reducing sugar monomer is released. Subsequent cleavage propagation from the levoglucosyl end of this chain will liberate levoglucosan (Figure 12).[4–6] This propagation continues down the polysaccharide chain releasing levoglucosan. Therefore, the initial cleavage at the end would release only one reducing sugar. Previous studies have also shown that glucose only generates around 10 wt % of levoglucosan during its primary fast pyrolysis because the dehydration of glucose to form levoglucosan is less kinetically and/or thermodynamically favored. Taken together, the formation of levoglucosan should be inversely proportional to the amount of reducing sugars formed during fast pyrolysis.

The weight percentage of reducing sugar in saccharides has been defined as the dextrose equivalent, and this value for glucose, cellobiose, and maltohexaose is 100%, 52%, and 18.2%, respectively. For cellulose, this value would approach zero because the DPs of all celluloses are much higher than for the short chain oligosaccharides. Given the relatively long polysaccharide chains in any type of cellulose, only minimal differences in dextrose equivalents would be observed among celluloses with different DP. As a result, the end effect, which

liberates the reducing end group thereby diminishing the formation of levoglucosan, would be negligible for different types of celluloses, and no difference in the pyrolytic yield of levoglucosan would be expected. Therefore, this mechanism could suggest that the evolution of levoglucosan would not be affected by the different DPs of glucose-based polysaccharides, which was consistent with the experimental results.

■ CONCLUSIONS

Primary reactions and secondary effects for cellulose fast pyrolysis were investigated in an online micropyrolyzer GC-MS/FID system by varying sample weight, particle size, and morphology of the cellulose sample. Prior to pyrolysis, all cellulose samples were proven to be essentially mineral free. Heating rate calculations suggested negligible heat transfer limitation for the cellulose pyrolysis system when an appropriate sample weight was used (<800 μg). It was found that mass transfer limitations dominated when excessive sample weight or sample particle length scale were applied, leading to a higher yield of gases and char and a lower yield of levoglucosan. That is, a greater amount of secondary reactions were observed for sample masses >800 μg and for when large cellulose domains were pyrolyzed. The changes in LMWs and furans yields observed for these cases could be attributed to different extents of secondary reactions. The mass transfer effects associated with secondary reactions were also observed when model compounds were copyrolyzed with char, which acted as a catalyst for secondary reactions. The secondary reactions include secondary char and gas formation from volatile products and decomposition and dehydration of levoglucosan into LMWs, furans, and dehydrated pyranose.

Fast pyrolysis of eight types of powder cellulose with different crystallinities, DPs, and feedstock sources was performed under well-controlled sample weight and particle size conditions. High mass balance closures were achieved for each case. Similar product distributions were observed for all eight types of cellulose, demonstrating that the primary reactions in the fast pyrolysis of cellulose were not affected by crystallinity, DP, or feedstock. The results suggested that H bonding and van der Waals forces do not play a significant role in the primary reactions of cellulose thermal deconstruction under fast pyrolysis conditions.

■ ASSOCIATED CONTENT

Ⓢ Supporting Information

Heat transfer estimation equations, cellulose and cellulose char mineral contents, EDS results for phase identification, pyrolysis product identification and calibration, HPLC of cellulose bio-oil, and detailed product distributions for cellulose at different sample weights, two types of thin film cellulose, the copyrolysis of cellulose and levoglucosan, levoglucosan and char, and celluloses from different feedstocks. Also included are selected product quantification of the copyrolysis of glycolaldehyde/5-HMF and char, as well as the statistical analysis for similarity for different celluloses. This material is available free of charge via the Internet at http://pubs.acs.org.

■ AUTHOR INFORMATION

Corresponding Author

*E-mail: bshanks@iastate.edu. Phone: +1 (515) 294 1895. Fax: +1 (515) 294 2689.

■ **REFERENCES**

(1) Huber, G. W.; Iborra, S.; Corma, A. Synthesis of transportation fuels from biomass: Chemistry, catalysts, and engineering. *Chem. Rev.* **2006**, *106*, 4044−4098.

(2) Klass, D. *Biomass for Renewable Energy, Fuels, and Chemicals*; Academic Press: Waltham, MA, 1998.

(3) Mettler, M. S.; Mushrif, S. H.; Paulsen, A. D.; Javadekar, A. D.; Vlachos, D. G.; Dauenhauer, P. J. Revealing pyrolysis chemistry for biofuels production: Conversion of cellulose to furans and small oxygenates. *Energy Environ. Sci.* **2012**, *5*, 5414−5424.

(4) Patwardhan, P. R.; Satrio, J. A.; Brown, R. C.; Shanks, B. H. Product distribution from fast pyrolysis of glucose-based carbohydrates. *J. Anal. Appl. Pyrolysis* **2009**, *86*, 323−330.

(5) Patwardhan, P. R.; Satrio, J. A.; Brown, R. C.; Shanks, B. H. Influence of inorganic salts on the primary pyrolysis products of cellulose. *Bioresour. Technol.* **2010**, *101*, 4646−4655.

(6) Vinu, R.; Broadbelt, L. J. A mechanistic model of fast pyrolysis of glucose-based carbohydrates to predict bio-oil composition. *Energy Environ. Sci.* **2012**, *5*, 9808−9826.

(7) Mayes, H. B.; Broadbelt, L. J. Unraveling the reactions that unravel cellulose. *J. Phys. Chem. A* **2012**, *116*, 7098−7106.

(8) Kato, K.; Komorita, H. Pyrolysis of cellulose. Part IV. Effect of crystallinity of cellulose on the formation of the volatile compounds. *Agric. Biol. Chem.* **1968**, *32*, 21−26.

(9) Bai, X.; Johnston, P.; Brown, R. C. An experimental study of the competing processes of evaporation and polymerization of levoglucosan in cellulose pyrolysis. *J. Anal. Appl. Pyrolysis* **2013**, *99*, 130−136.

(10) Varhegyi, G.; Antal, M. J.; Szekely, T.; Till, F.; Jakab, E. Simultaneous thermogravimetric-mass spectrometric studies of the thermal decomposition of biopolymers. 1. Avicel cellulose in the presence and absence of catalysts. *Energy Fuels* **1988**, *2*, 267−272.

(11) Antal, M. J.; Varhegyi, G.; Jakab, E. Cellulose pyrolysis kinetics: Revisited. *Ind. Eng. Chem. Res.* **1998**, *37*, 1267−1275.

(12) Lin, Y. C.; Cho, J.; Tompsett, G. A.; Westmoreland, P. R.; Huber, G. W. Kinetics and mechanism of cellulose pyrolysis. *J. Phys. Chem. C* **2009**, *113*, 20097−20107.

(13) Patwardhan, P. R.; Dalluge, D. L.; Shanks, B. H.; Brown, R. C. Distinguishing primary and secondary reactions of cellulose pyrolysis. *Bioresour. Technol.* **2011**, *102*, 5265−5269.

(14) Paulsen, A. D.; Mettler, M. S.; Dauenhauer, P. J. The role of sample dimension and temperature in cellulose pyrolysis. *Energy Fuels* **2013**, *27*, 2126−2134.

(15) Mettler, M. S.; Paulsen, A. D.; Vlachos, D. G.; Dauenhauer, P. J. Pyrolytic conversion of cellulose to fuels: levoglucosan deoxygenation via elimination and cyclization within molten biomass. *Energy Environ. Sci.* **2012**, *5*, 7864−7868.

(16) Ott, E.; Spurlin, H. M.; Grafflin, M. W. *Cellulose and Cellulose Derivatives*, 2nd ed.; Interscience Publishers, Inc.: New York, 1954.

(17) Klemm, D.; Heublein, B.; Fink, H.-P.; Bohn, A. Cellulose: Fascinating biopolymer and sustainable raw material. *Angew. Chem., Int. Ed.* **2005**, *44*, 3358−3393.

(18) Gurgel, L. V. A.; Marabezi, K.; Ramos, L. A.; da Silva Curvelo, A. A. Characterization of depolymerized residues from extremely low acid hydrolysis (ELA) of sugarcane bagasse cellulose: Effects of degree of polymerization, crystallinity and crystallite size on thermal decomposition. *Ind. Crops Prod.* **2012**, *36*, 560−571.

(19) Poletto, M.; Pistor, V.; Zeni, M.; Zattera, A. J. Crystalline properties and decomposition kinetics of cellulose fibers in wood pulp obtained by two pulping processes. *Polym. Degrad. Stab.* **2011**, *96*, 679−685.

(20) Schultz, T. P.; McGinnis, G. D.; Nicholas, D. D. Effect of Crystallinity and Additives on the Thermal Degradation of Cellulose. In *Fire and Polymers*; Nelson, G. L., Ed.; ; ACS Symposium Series 425; American Chemical Society: Washington, DC, 1990; pp 335−360.

(21) Kim, U.-J.; Eom, S. H.; Wada, M. Thermal decomposition of native cellulose: Influence on crystallite size. *Polym. Degrad. Stab.* **2010**, *95*, 778−781.

(22) Shimazu, F.; Sterling, C. Effect of wet and dry heat on structure of cellulose. *J. Food Sci.* **1966**, *31*, 548−551.

(23) Wang, Z.; McDonald, A. G.; Westerhof, R. J.; Kersten, S. R.; Cuba-Torres, C. M.; Ha, S.; Pecha, B.; Garcia-Perez, M. Effect of cellulose crystallinity on the formation of a liquid intermediate and on product distribution during pyrolysis. *J. Anal. Appl. Pyrolysis* **2013**, *100*, 56−66.

(24) Zhang, Y.-H. P.; Cui, J.; Lynd, L. R.; Kuang, L. R. A transition from cellulose swelling to cellulose dissolution by o-phosphoric acid: Evidence from enzymatic hydrolysis and supramolecular structure. *Biomacromolecules* **2006**, *7*, 644−648.

(25) Sieder, E. N.; Tate, G. E. Heat transfer and pressure heat transfer and pressure drop of liquids in tubes. *Ind. Eng. Chem.* **1936**, *28*, 1429−1435.

(26) Incropera, F. P.; DeWitt, D. P. *Fundamentals of Heat and Mass Transfer*, 6th ed.; Wiley: New York, 2007.

(27) Oja, V.; Suuberg, E. M. Vapor pressures and enthalpies of sublimation of d-glucose, d-xylose, cellobiose, and levoglucosan. *J. Chem. Eng. Data* **1999**, *44*, 26−29.

(28) Verevkin, S. P.; Emelýanenko, V. N.; Stepurko, E. N.; Ralys, R. V.; Zaitsau, D. H.; Stark, A. Biomass-derived platform chemicals: Thermodynamic studies on the conversion of 5-hydroxymethylfurfural into bulk intermediates. *Ind. Eng. Chem. Res.* **2009**, *48*, 10087−10093.

(29) Petitjean, M.; Reyès-Pérez, E.; Pérez, D.; Mirabel, P.; Le Calvé, S. Vapor pressure measurements of hydroxyacetaldehyde and hydroxyacetone in the temperature range (273 to 356) K. *J. Chem. Eng. Data* **2010**, *55*, 852−855.

(30) Perry, R. H., Green, D. W., Maloney, J. O., Eds. *Perry's Chemical Engineering Handbook*, 6th ed.; McGraw-Hill: New York, 1984.

(31) Park, S.; Baker, J. O.; Himmel, M. E.; Parilla, P. A.; Johnson, D. K. Cellulose crystallinity index: measurement techniques and their impact on interpreting cellulase performance. *Biotechnol. Biofuels* **2010**, *3*, 10.

(32) Thygesen, A.; Oddershede, J.; Lilholt, H.; Thomsen, A. B.; Ståhl, K. On the determination of crystallinity and cellulose content in plant fibres. *Cellulose* **2005**, *12*, 563−576.

(33) Hermans, P. H. *Physics and Chemistry of Cellulose Fibres, with Particular Reference to Rayon*; Elsevier: Amsterdam, The Netherlands, 1949.